IEEE Control Systems Letters paper presented at
2023 62nd IEEE Conference on Decision and Control (CDC)
December 13-15, 2023. Marina Bay Sands, Singapore

Time-Fuel-Optimal Navigation of a Commercial Aircraft in Cruise with Heading and Throttle Controls using Pontryagin's Maximum Principle

Amin Jafarimoghaddam, and Manuel Soler

***Abstract*—In this letter, we consider the commercial aircraft trajectory optimization problem for a general cruise model with arbitrary spatial wind fields to be solved using the Pontryagin's maximum principle. The model features two fundamental controls, namely "throttle setting" (appearing as a singular control) and "heading angle" (appearing as a regular control). For a problem with state-inequality constraints and minimum time-fuel objective, we show that the optimal "heading angle" can be described through the classic Zermelo's navigation identity. We also demonstrate, by analyzing the switching function, that the singular "throttle setting" can be characterized through a feedback function that relies on both the optimal states and "heading angle". The switching-point algorithm is employed to solve a case study where we inspect the optimality conditions and graph the optimal controls together with the optimal state and co-state variables.**

***Index Terms*—Complete Cruise model, Two active controls, Indirect optimization**

I. Introduction

The optimization of commercial aircraft trajectories has been the subject of extensive research, with a variety of optimization techniques having been applied, however, the Pontryagin's maximum principle, has received comparatively little attention in the literature [1].

Focusing only on those approaches using the Pontryagin's maximum principle, the commercial aircraft navigation problem in the cruise phase with various cost functions has been solved in [2]–[8]. More specifically, the range-optimal problem has been solved in [2]. The same problem was revisited w.r.t. the compressibility effects in [3]. Also, the fuel-optimal cruise at constant altitude with fixed arrival time has been solved in [4]. Likewise, the fuel-optimal problem in a vertical plane (including the cruise phase) has been solved for structured flight segments in [5]. The fuel-optimal problem in the cruise phase with a one-dimensional uniform wind field and fixed arrival time has been solved in [6]. In the literature, there are additional studies that take climate impact into consideration, as exemplified by [7]. In this study, the problem of contrails avoidance during the cruise phase was addressed. However, it is important to note that the approach presented in [7] does not account for the dynamics of speed and the derivative of the Hamiltonian w.r.t. the aircraft's mass. Despite this limitation, the study in [7] provides a more general navigation formula. Furthermore, the issue of direct operating cost with multiple cruise altitudes in the presence of wind is discussed in [8]. It should be mentioned, however, that similar to [7], the study in [8] also does not consider speed dynamics.

To summarize, the reviewed literature ([2]–[8]) mainly focuses on simplified cruise models with only one active control (either "throttle setting", or "heading angle"). However, solving the optimal control problem associated with a general cruise model using the Pontryagin's maximum principle is particularly challenging due to the involvement of the two controls. In this research, we tackle this challenge and solve the problem for the first time.

In this research, we consider a generic (realistic) cruise model, comprising of two active controls. The controls are: 1) the heading angle (a regular control), and, 2) the throttle setting (a singular control). The objective is to minimize the direct operating cost. We show that the optimal heading angle is fully characterized through the classic Zermelo's navigation identity even if the problem is subject to some standard state-inequality constraints (the classic Zermelo's navigation identity is the time-optimal, constant-speed navigation problem between two points inside a fluid flow [9]). To determine the singular throttle setting, we exploit the successive time-derivatives of the switching function and leverage the optimality information related to the heading angle. This approach enables us to define the singular control as a complete feedback function. By analyzing the switching function, we establish that the singular throttle setting is dependent on the optimal heading angle. The derived formula that captures this dependency offers valuable analytical insights into the behavior of the optimal controls within a realistic cruise model.

The switching-point algorithm [10] is employed to solve a case study where the state-inequality constraints are inactive. In short, the switching-point algorithm runs a nonlinear programming only over the switching times and (possibly) some other parameters with a given control feedback. The switching-point algorithm, as in [10], is for a singular control problem without state-inequality constraints. It is noteworthy that [10] is an extension to the previous works in this discipline (see e.g., [11] and [12]).

II. Problem Statement

The point-mass dynamics are commonly used to generate aircraft trajectories [13], [14]. For commercial aircraft flights

This paragraph of the first footnote will contain the date on which you submitted your paper for review.

Amin Jafarimoghaddam, and Manuel Soler are with the Department of Aerospace Engineering, Universidad Carlos III de Madrid, Leganes, Madrid, Spain (email: ajafarim@pa.uc3m.es; masolera@ing.uc3m.es)

in cruise phase, the point-mass equations in Cartesian framework can be approximated as [15]:

$$\begin{aligned}
\frac{dx}{dt} &= v(t)\cos(\chi(t)) + w_x(x(t),y(t),h) =: F_x,\\
\frac{dy}{dt} &= v(t)\sin(\chi(t)) + w_y(x(t),y(t),h) =: F_y,\\
\frac{dv}{dt} &= \frac{\Pi(t)T_{max}(h) - D(m(t),v(t),h)}{m(t)} =: F_v,\\
\frac{dm}{dt} &= -\Pi(t)C_s(v(t))T_{max}(h) =: F_m.
\end{aligned} \tag{1}$$

In Eq. (1), x, and y are geometric variables, i.e., the cruise flight occurs in a horizontal $x-y$ plane, v is the aerodynamic speed, m is the aircraft mass, and t is time. In addition, w_x and w_y are x, and y components of wind respectively (w_x and w_y are known geometrical functions), h is a constant altitude where the cruise flight occurs, T_{max} is the maximum thrust force, D is the drag force, and C_s is the fuel flow. The controls are the heading angle ($\chi(t)$) and the throttle setting ($\Pi(t)$).

The objective is the direct operating cost (i.e., a combination of the arrival time and fuel burn):

$$\min_{\chi(t),\Pi(t),t_f} \mathcal{J} = \alpha t_f + (\alpha-1)m(t_f), \quad 0 \le \alpha \le 1, \tag{2}$$

where t_f denotes the final time.

The cruise flight envelope is defined by the dynamic constraints described in Eq. (1) , along with the following set of standard state-inequality constraints that hold $\forall t \in [t_0, t_f]$:

$$\begin{aligned}
&M_{min} \le M(h,v(t)) \le M_{max},\\
&v_{CAS,min} \le v_{CAS}(h,v(t)) \le v_{CAS,max},
\end{aligned} \tag{3}$$

and boundary conditions:

$$\begin{aligned}
&x(t_0) = x_0, \quad y(t_0) = y_0, \quad v(t_0) = v_0, \quad m(t_0) = m_0,\\
&x(t_f) = x_f, \quad y(t_f) = y_f, \quad v(t_f) = v_f.
\end{aligned} \tag{4}$$

In above, t_0 is the initial time, M is the $Mach$ number, and v_{CAS} is the calibrated airspeed [16].

The controls are also constrained $\forall t \in [t_0, t_f]$ as:

$$\Pi_{min} \le \Pi(t) \le \Pi_{max}, \quad \chi_{min} \le \chi(t) \le \chi_{max}. \tag{5}$$

It is noteworthy that, for the succeeding analysis, only the functionality of w_x, w_y, T_{max}, D, C_s, $Mach$, and V_{CAS} is of relevance. Nonetheless, these terms will be elaborated in our case study (see sec.IV).

A. Compact Form Notation

The optimal control problem considered, can be written in a compact form notation as:

$$\begin{aligned}
&\min_{U(t),t_f} \mathcal{J} = \Phi(X_f, t_f),\\
&s.t.,\\
&\frac{dX}{dt} = F(X,U),\\
&\mathcal{C}(U) \le 0, \quad \mathcal{S}(X) \le 0, \quad \forall t \in [t_0, t_f],\\
&\phi_0(X_0) = 0, \quad \phi_f(X_f) = 0.
\end{aligned} \tag{6}$$

where $X^T = [x(t), y(t), v(t), m(t)]$, $F^T = [F_x, F_y, F_v, F_m]$, $\phi_0(X_0) = X_0 - X(t_0)$, $\phi_0 \in \mathbb{R}^4$, $\phi_f(X_f) = X_f - X(t_f)$, $\phi_f \in \mathbb{R}^3$, $U^T = [\chi(t), \Pi(t)]$, and $\Phi(X_f, t_f) = \alpha t_f + (\alpha-1)m(t_f)$. The inequality constraints are:

$$\mathcal{C}(U) = \begin{pmatrix} \chi(t) - \chi_{max} \\ \chi_{min} - \chi(t) \\ \Pi(t) - \Pi_{max} \\ \Pi_{min} - \Pi(t) \end{pmatrix}, \tag{7}$$

$$\mathcal{S}(X) = \begin{pmatrix} M(t) - M_{max} \\ M_{min} - M(t) \\ v_{CAS}(t) - v_{CAS,max} \\ v_{CAS,min} - v_{CAS}(t) \end{pmatrix}. \tag{8}$$

By directly adjoining the constraints, we can define an augmented cost as (see e.g. [17]):

$$\begin{aligned}
&\bar{\mathcal{J}} := \Phi(X_f,t_f) + \langle \nu_0, \phi_0(X_0)\rangle + \langle \nu_f, \phi_f(X_f)\rangle +\\
&\int_{t_0}^{t_f} \Big(\langle \lambda, F(X,U) - \frac{dX}{dt}\rangle + \langle \mu, \mathcal{C}(U)\rangle + \langle \eta, \mathcal{S}(X)\rangle \Big) dt.
\end{aligned} \tag{9}$$

In above, the scalar multipliers are denoted by $\nu_0 \in \mathbb{R}^4$, and $\nu_f \in \mathbb{R}^3$, while the inequality multipliers are represented by $\mu^T = [\mu_u^\chi(t), \mu_l^\chi(t), \mu_u^\Pi(t), \mu_l^\Pi(t)]$, and $\eta : [t_0, t_f] \to \mathbb{R}^4$. Additionally, the co-states are given by $\lambda^T = [\lambda_x(t), \lambda_y(t), \lambda_v(t), \lambda_m(t)]$.

For this optimal control problem, the Hamiltonian ($\mathcal{H} := \mathcal{H}(X,U,\lambda,\mu,\eta)$) is defined as [17]:

$$\mathcal{H} = \langle \lambda, F(X,U)\rangle + \langle \mu, \mathcal{C}(U)\rangle + \langle \eta, \mathcal{S}(X)\rangle. \tag{10}$$

The optimality conditions ($\forall t \in [t_0, t_f]$) are:

$$\frac{\partial \mathcal{H}}{\partial U} = 0, \quad \langle \mu, \mathcal{C}(U)\rangle = 0, \quad \langle \eta, \mathcal{S}(X)\rangle = 0. \tag{11}$$

where $\mu \ge 0, \eta \ge 0$, $\forall t \in [t_0, t_f]$. The co-state dynamics and the transversality conditions read:

$$\begin{aligned}
&\frac{d\lambda^T}{dt} = -\frac{\partial \mathcal{H}}{\partial X},\\
&\lambda(t_0) = -\big[\frac{\partial \phi_0}{\partial X_0}\big]^T \nu_0,\\
&\lambda(t_f) = \frac{\partial \Phi}{\partial X_f} + \big[\frac{\partial \phi_f}{\partial X_f}\big]^T \nu_f,\\
&\mathcal{H}(t_f) = -\frac{\partial \Phi}{\partial t_f} - \nu_f^T \frac{\partial \phi_f}{\partial t_f}.
\end{aligned} \tag{12}$$

Let τ be a possible time instant within the state-boundary arc at which the co-state variables are discontinuous. The jump conditions at the junction times read [18]:

$$\begin{aligned}
&\lambda^T(\tau^-) = \lambda^T(\tau^+) - \nu^T(\tau) \frac{\partial \mathcal{S}}{\partial X}|_{t=\tau},\\
&\nu(\tau) \ge 0, \quad \langle \nu(\tau), \mathcal{S}(X(\tau))\rangle = 0.
\end{aligned} \tag{13}$$

Since the state-inequality constraints (see Eq. (8)) are functions of $v(t)$, it is straightforward to show that the jump condition (upon existence), applies only to $\lambda_v(t)$.

III. Classification of the Controls

The control problem defined through Eq. (1) to Eq. (5) is regular on the heading angle ($\chi(t)$), and singular on the throttle setting ($\Pi(t)$). In order to classify the controls, we write:

$$F(X,\chi(t),\Pi(t)) = Q(X,\chi(t)) + \Pi(t)P(X). \tag{14}$$

In above,

$$Q(X,\chi(t)) = \begin{pmatrix} v(t)\cos(\chi(t)) + w_x(x(t),y(t),h) \\ v(t)\sin(\chi(t)) + w_y(x(t),y(t),h) \\ -\frac{D(m(t),v(t),h)}{m(t)} \\ 0 \end{pmatrix}, \tag{15}$$

and,

$$P(X) = \begin{pmatrix} 0 \\ 0 \\ \frac{T_{max}(h)}{m(t)} \\ -C_s(v(t))T_{max}(h) \end{pmatrix}. \tag{16}$$

A. The Optimal $\chi(t)$ (Heading Angle)

The optimal $\chi(t)$, associated with the interior arc ($\mu_l^{\chi}(t) = \mu_u^{\chi}(t) = 0$), is obtained as:

$$\frac{\partial \mathcal{H}}{\partial \chi} = 0 \rightarrow \langle \lambda, \frac{\partial Q}{\partial \chi} \rangle = 0 \rightarrow \tan(\chi(t)) = \frac{\lambda_y(t)}{\lambda_x(t)}. \tag{17}$$

From Eq. (12), the co-state dynamics $\frac{d\lambda_y}{dt}$, and $\frac{d\lambda_x}{dt}$ can be written as:

$$\begin{aligned} \frac{d\lambda_x}{dt} &= -\big(\lambda_x(t)\frac{\partial w_x}{\partial x} + \lambda_y(t)\frac{\partial w_y}{\partial x}\big), \\ \frac{d\lambda_y}{dt} &= -\big(\lambda_x(t)\frac{\partial w_x}{\partial y} + \lambda_y(t)\frac{\partial w_y}{\partial y}\big). \end{aligned} \tag{18}$$

Importantly, the co-state dynamics mentioned above do not involve the multipliers η, since the state-inequality constraints are solely functions of $v(t)$. Differentiating Eq. (17) w.r.t. time, and with the help of Eq. (18), we obtain:

$$\begin{aligned} &\frac{d\chi}{dt}\big(1+\tan^2(\chi(t))\big) = -\frac{\partial w_x}{\partial y} + \\ &\big(\frac{\partial w_x}{\partial x} - \frac{\partial w_y}{\partial y}\big)\tan(\chi(t)) + \big(\frac{\partial w_y}{\partial x}\big)\tan^2(\chi(t)). \end{aligned} \tag{19}$$

We observe that this equation is the Zermelo's navigation identity [9]; however, now it defines the optimal $\chi(t)$ for a more general control problem even with active state-inequality constraints.

B. The Optimal $\Pi(t)$ (Throttle Setting)

Let us assume that the state-inequality constraints are inactive, i.e., $\eta = 0, \forall t \in [t_0, t_f]$.

The first-order optimality condition for $\Pi(t)$ reads:

$$\frac{\partial \mathcal{H}}{\partial \Pi} = 0 \rightarrow \langle \lambda, P(X) \rangle + \mu_u^{\Pi}(t) - \mu_l^{\Pi}(t) = 0. \tag{20}$$

We define the switching function as:

$$S(t) = \langle \lambda, P(X) \rangle. \tag{21}$$

The bang-singular classification for the optimal $\Pi(t)$ is:

$$\Pi(t) = \begin{cases} \Pi_{min} & S(t) > 0, \\ \Pi_{max} & S(t) < 0, \\ \text{undetermined (singular)} & S(t) = 0. \end{cases} \tag{22}$$

For the singular $\Pi(t)$, since $S(t) = 0$, we have: $S^{(k)}(t) := \frac{d^k}{dt^k}S(t) = 0, k = 1, 2, ...$ It can be checked that the singular $\Pi(t)$ appears in $S^{(2)}(t)$; that is to say, order of the singular arc is one. Since the Hamiltonian is not an explicit function of time, we have: $\mathcal{H} = constant$ ($\forall t \in [t_0, t_f]$). Therefore, from Eq. (12), we have: $\mathcal{H} = -\alpha$. Moreover, $\frac{\partial \mathcal{H}}{\partial \chi} = 0$ holds at all times.

On using Eq. (14), the co-state dynamics can be written as:

$$\frac{d\lambda^T}{dt} = -\lambda^T\big(\frac{\partial Q}{\partial X} + \Pi(t)\frac{\partial P}{\partial X}\big). \tag{23}$$

The first time-derivative of the switching function is computed as:

$$S^{(1)}(t) = \langle \frac{d\lambda}{dt}, P(X) \rangle + \langle \lambda, \frac{dP}{dt} \rangle = 0. \tag{24}$$

Noting that $\frac{dP}{dt} = \frac{\partial P}{\partial X}\frac{dX}{dt}$, it is straightforward to show that $\Pi(t)$ drops from $S^{(1)}(t)$. As a result, $S^{(1)}(t)$ can be expressed as follows:

$$S^{(1)}(t) = \langle \lambda, \mathcal{A}(X,\chi(t)) \rangle. \tag{25}$$

In Eq. (25), the vector $\mathcal{A}$ is as follows:

$$\mathcal{A}(X,\chi(t)) = \frac{\partial P}{\partial X}Q(X,\chi(t)) - \frac{\partial Q}{\partial X}P(X). \tag{26}$$

It should be noted that the vector $\mathcal{A}$ can also be represented using Lie bracket notations.

We exploit the following set of algebraic equations to express the co-states in explicit terms:

$$\begin{aligned} &S(t) = 0 \rightarrow \langle \lambda, P(X) \rangle = 0, \\ &S^{(1)}(t) = 0 \rightarrow \langle \lambda, \mathcal{A}(X,\chi(t)) \rangle = 0, \\ &\mathcal{H} = -\alpha \rightarrow \langle \lambda, Q(X,\chi(t)) \rangle = -\alpha, \\ &\frac{\partial \mathcal{H}}{\partial \chi} = 0 \rightarrow \langle \lambda, \frac{\partial Q}{\partial \chi} \rangle = 0. \end{aligned} \tag{27}$$

The above algebraic linear system can be simply solved by any platform supporting symbolic computations such as MATLAB. To this end, we write the solution to system (27) as:

$$\det[\bar{\bar{\mathcal{M}}}] \begin{pmatrix} \lambda_x(t) \\ \lambda_y(t) \\ \lambda_v(t) \\ \lambda_m(t) \end{pmatrix} = adj[\bar{\bar{\mathcal{M}}}]\mathcal{R}. \tag{28}$$

where,

$$\bar{\bar{\mathcal{M}}} = \begin{pmatrix} 0 & 0 & P_3 & P_4 \\ \mathcal{A}_1 & \mathcal{A}_2 & \mathcal{A}_3 & \mathcal{A}_4 \\ Q_1 & Q_2 & Q_3 & 0 \\ \tan(\chi(t)) & -1 & 0 & 0 \end{pmatrix}, \mathcal{R} = \begin{pmatrix} 0 \\ 0 \\ -\alpha \\ 0 \end{pmatrix}. \tag{29}$$

In Eq. (29), subscripts denote the vector elements.

In order to obtain the optimal singular $\Pi(t)$, we write:

$$S^{(2)}(t) = \langle \frac{d\lambda}{dt}, \mathcal{A}(X, \chi(t)) \rangle + \langle \lambda, \frac{d\mathcal{A}}{dt} \rangle = 0. \tag{30}$$

The time-derivative of the vector $\mathcal{A}$ is computed as:

$$\frac{d\mathcal{A}}{dt} = \frac{\partial \mathcal{A}}{\partial X}\frac{dX}{dt} + \frac{\partial \mathcal{A}}{\partial \chi}\frac{d\chi}{dt}. \tag{31}$$

With Eq. (30), Eq. (31), and Eq. (23)), one arrives at:

$$S^{(2)}(t) = 0 \rightarrow \Pi(t) = -\frac{\langle \lambda, \mathcal{B} \rangle + \langle \lambda, \frac{\partial \mathcal{A}}{\partial \chi} \rangle \frac{d\chi}{dt}}{\langle \lambda, \mathcal{D} \rangle}. \tag{32}$$

where,

$$\begin{aligned} \mathcal{B} &= \frac{\partial \mathcal{A}}{\partial X} Q(X, \chi(t)) - \frac{\partial Q}{\partial X} \mathcal{A}(X, \chi(t)), \\ \mathcal{D} &= \frac{\partial \mathcal{A}}{\partial X} P(X) - \frac{\partial P}{\partial X} \mathcal{A}(X, \chi(t)). \end{aligned} \tag{33}$$

The generalized Legendre-Clebsch (LC) second-order necessary conditions dictate [19]:

$$-\langle \lambda, \mathcal{D} \rangle \geq 0, \quad \forall t \in \Omega_s. \tag{34}$$

where Ω_s is an interval where the optimal $\Pi(t)$ is singular.

It is worth noting that, in the current study, all computations associated with the optimal $\chi(t)$ and singular $\Pi(t)$ were carried out symbolically in MATLAB. This involved solving the co-state system defined by Eq. (28) and deriving symbolic formulas for the vectors $\mathcal{A}$, $\mathcal{B}$, and $\mathcal{D}$.

1) The Special Case $\alpha = 0$: Since $\mathcal{R} = \vec{0}$ if $\alpha = 0$, the solution to Eq. (28) becomes intractable. On this occasion, from Eq. (28), we have:

$$\det\left[\bar{\bar{\mathcal{M}}}\right] = 0 \rightarrow \frac{d}{dt} \det\left[\bar{\bar{\mathcal{M}}}\right] = 0. \tag{35}$$

Therefore, from Eq. (35), we obtain the singular $\Pi(t)$ as:

$$\Pi(t) = -\frac{\frac{\partial}{\partial X} \det\left[\bar{\bar{\mathcal{M}}}\right] Q(X(t), \chi(t))}{\frac{\partial}{\partial X} \det\left[\bar{\bar{\mathcal{M}}}\right] P(X(t))}. \tag{36}$$

It is noteworthy that we can also handle the case $\alpha = 0$ asymptotically, i.e., to compute for $\alpha \rightarrow 0$.

IV. Case Study

In accordance with our analysis presented in the previous sections, we consider inequality constraints only w.r.t. the throttle setting, i.e., $\Pi_{min} \leq \Pi(t) \leq \Pi_{max}, \forall t \in [0, t_f]$.

We use the BADA3 model for $T_{max}(h)$, $C_s(v)$, and $D(m, v, h)$ [20]. In addition, air density is approximated by International Standard Atmospheric (ISA) model:

$$\begin{aligned} &T_{max}(h) = C_{T_1}\big(1 - \frac{h}{C_{T_2}} + h^2 C_{T_3}\big), C_s(v) = C_{s_1}\big(1 + \frac{v}{C_{s_2}}\big), \\ &P(h) = P_0\big(\frac{\Theta_0 - \beta h}{\Theta_0}\big)^{\frac{g}{\beta R}}, \quad \rho(h) = \frac{P(h)}{R(\Theta_0 - \beta h)}, \\ &D(m, v, h) = \frac{1}{2}\rho(h) s v^2 \big(C_{D_1} + C_{D_2} C_l^2\big), C_l = \frac{2mg}{\rho s v^2}. \end{aligned} \tag{37}$$

In above, s is the aerodynamic lift surface and ρ is the air density. $C_{T_i}, i = 1, 2, 3$, s, $C_{D_i}, i = 1, 2$, $C_{s_i}, i = 1, 2$, R, β, P_0, g, and Θ_0 are known constants for a medium-haul aircraft (see [16] for a quick access to their specific values and definitions). Since h is a constant (i.e., the cruise altitude), the maximum thrust force $T_{max}(h)$ will be a constant too.

The wind components are simulated by a general second-order polynomial for each component.

Without loss of generality, we can consider $w_x = w_x(x, y)$, and $w_y = w_y(x, y)$, and drop h. We also note that the vertical component of wind is assumed to be zero [15], [13]. Therefore, for the sake of consistency with the fluid flow behavior, the continuity equation must be satisfied, i.e., $\frac{\partial w_x}{\partial x} + \frac{\partial w_y}{\partial y} = 0$. With this observation, the wind components become:

$$\begin{aligned} &w_x(x, y) = (a_0 \bar{w}_x^b) + (a_1 \frac{\bar{w}_x^b}{x_f})x + (a_2 \frac{\bar{w}_x^b}{x_f^2})x^2 + \\ &(a_3 \frac{\bar{w}_x^b}{y_f})y + (a_4 \frac{\bar{w}_x^b}{y_f^2})y^2 + (a_5 \frac{\bar{w}_x^b}{x_f y_f})xy, \\ &w_y(x, y) = -\int \frac{\partial w_x}{\partial x} dy + f(x), \\ &f(x) = \bar{w}_y^b + (b_0 \frac{\bar{w}_y^b}{x_f})x + (b_1 \frac{\bar{w}_y^b}{x_f^2})x^2. \end{aligned} \tag{38}$$

In above, $a_i, i = 0, .., 5$, and $b_i, i = 0, 1$ are in general dimensionless random values between -1 and $+1$. Moreover, $\bar{w}_x^b$, and $\bar{w}_y^b$ are average dimensional wind constants.

Upon conducting an estimation of real wind data (w.r.t. various, though small, atmospheric zones) using the above wind model, we observed a very good level of consistency. In particular, the total modeling error for the wind components was found to be below 10 percent in relation to low-resolution wind data. However, in this study, we adopt a generalized approach and do not fine-tune the model based on specific data sets. The tabulated parameters in Table (I) are those we have fixed in our simulations. Therefore, one can check that the only free parameter in our simulations is α.

TABLE I
BOUNDARY CONDITIONS, BOUNDS, AND THE SELECTED SNAPSHOT OF THE WIND PARAMETERS

x_0	$0(m)$	x_f	$1.5\times10^6(m)$
y_0	$0(m)$	y_f	$7\times10^5(m)$
v_0	$200(m/s)$	v_f	$200(m/s)$
m_0	$59000(kg)$	h	$10000(m)$
Π_{max}	1	Π_{min}	0
$\bar{w}_x^b$	$40(m/s)$	$\bar{w}_y^b$	$-20(m/s)$
a_0	0.77406	a_1	-0.86240
a_2	-0.63294	a_3	0.47414
a_4	0.39342	a_5	0.55398
b_0	0.00380	b_1	-0.14900

V. Computational Algorithm

Preliminary analysis (using a single-shooting Euler-based direct transcription method with high number of grids) implies that the optimal $\Pi(t)$ contains at most one (interior) singular arc between two boundary arcs.

We have employed the switching-point algorithm, taking the switching times and the initial heading as decision variables

(see [10] for more information about the switching-point algorithm and the associated mathematical justifications). More specifically, we extend the state dynamics by Eq. (19), and the nonlinear programming becomes:

$$
\begin{aligned}
&\min_{\chi(0),t_1,t_2,t_f} \hat{\mathcal{J}} = \Phi(X_f, t_f),\\
&s.t.,\\
&\frac{dX}{dt} = F(X(t), \chi(t), \Pi(t)),\\
&\frac{d\chi}{dt}\big(1+\tan(\chi(t))^2\big) = -\frac{\partial w_x}{\partial y} +\\
&\big(\frac{\partial w_x}{\partial x} - \frac{\partial w_y}{\partial y}\big)\tan(\chi(t)) + \big(\frac{\partial w_y}{\partial x}\big)\tan(\chi(t))^2, \qquad (39)\\
&\phi_0(X_0) = 0, \quad \phi_f(X_f) = 0,\\
&0 \le t_1 \le t_2 \le t_f,\\
&\Pi(t) = \begin{cases} \Pi_{max} & t \in [0, t_1),\\ Eq.(32) \vee Eq.(36) & t \in [t_1, t_2],\\ \Pi_{min} & t \in (t_2, t_f]. \end{cases}
\end{aligned}
$$

We have adopted the interior-point/barrier algorithm of the nonlinear programming solver $fmincon$ from MATLAB® Optimization Toolbox as the optimization module.

We use the results due to the above nonlinear programming to compute the co-state variables (and accordingly, the switching function) over the boundary arcs. This is doable by backward and forward integration of the co-state dynamics from t_1, and t_2 respectively.

A. Special Case with a Constant Wind Field

Assuming a constant wind field, it is demonstrated that the optimization problem formulated in Eq. (39) can exclude $\chi(0)$ as a decision variable.

Suppose that $w_x = constant =: W_x$, and $w_y = constant =: W_y$.

From the system dynamics Eq. (1), we can write:

$$\frac{dx}{dt} = v(t)\cos(\chi(t)) + W_x, \quad \frac{dy}{dt} = v(t)\sin(\chi(t)) + W_y. \qquad (40)$$

Since W_x, and W_y are constants, from Eq. (19) we have: $\chi(t) = \chi(0) = constant$. Therefore, by integrating Eq. (40) from 0 to t_f, and after some manipulations, we get:

$$\tan(\chi(0)) = \frac{y_f - W_y t_f - y_0}{x_f - W_x t_f - x_0}. \qquad (41)$$

Therefore, in case of having a constant wind field, the initial heading angle $\chi(0)$ is a function of the constant wind components, boundary conditions, and the final time t_f.

VI. Numerical Results

We have obtained optimal results for various values of α. From the definition of the cost function, α determines the trade-off between fuel-optimal and time-optimal problems. For each studied α, we have checked the second-order optimality condition (Eq. (34)) for the singular arc and the first-order optimality condition for the boundary arcs. In addition, for each stage of α, we have compared our results with the results due to a single-shooting Euler-based direct transcription method with high number of grids (see e.g., Fig. 1-**a**). The results of our study reveal a noteworthy similarity between the optimal costs obtained from the direct method and the current indirect method. However, it is important to note that the direct transcription method, in contrast to the indirect method, exhibits a chattering solution for the singular arc.

Moreover, we note that the switching-point algorithm does not directly account for $\lambda(t_f)$. From the transversality conditions, we can check that $\lambda_m(t_f) = \alpha - 1$. By computing the co-state variables over the boundary arcs (after nonlinear programming), we have checked that $|\lambda_m(t_f) - (\alpha - 1)| < 10^{-4}$. This also stands as an additional confirmation of the obtained optimal results (see Fig. 2-**d**).

The optimal controls $\Pi(t)$, $\chi(t)$, and the optimal states ($m(t)$ as a function of $v(t)$) are shown in Fig. 1-**b**, Fig. 1-**c**, and Fig. 1-**d** respectively. Based on Fig. 1-**b** and Fig. 1-**d**, it is clear that an increase in α leads to a corresponding increase in the optimal speed by adjusting the throttle setting.

From Fig. 1-**b**, it can be observed that as α increases, the first "bang" segment of the optimal throttle $\Pi(t)$ expands. This implies that there is a specific value of α at which the optimal $\Pi(t)$ switches to a "bang-bang" control.

The optimal co-state variables in different values of α are graphed in Fig. 2-**a** to Fig. 2-**d**.

As depicted in Fig. 2-**d**, $\lambda_m(t)$ displays only marginal changes with respect to time. Consequently, it might be deemed logical to treat it as a constant during the examination of the optimality conditions, particularly in engineering applications where rough approximations of optimality are sufficient.

Fig. 3 illustrates the impact of α on the optimal $x - y$ trajectories. Upon examination of the figure, it is apparent that the parameter α exhibits negligible influence on the evolution of the $x - y$ trajectories. More precisely, the $x - y$ trajectories are more contingent on the wind configuration.

VII. Conclusion and Future Works

Pontryagin's maximum principle was applied to solve a general (realistic) version of the optimization problems related to commercial aircraft trajectory in cruise phase. The analysis focused on the control functions, from which optimality formulas were derived. To handle the singular control, the switching-point algorithm was utilized as an alternative approach to the conventional shooting methods. Regarding computational time, our simulations reveal that the presented indirect approach outperforms direct transcription methods significantly, especially when the solution structure is already known. Remarkably, an identified solution structure remains consistent across a broad range of modeling parameters. Based on the numerical findings, an open line of research for further investigation is to examine the condition (w.r.t. α) under which the singular $\Pi(t)$ vanishes. Additionally, it is worth noting that our case study did not incorporate state-inequality constraints, which presents another potential area for future research.

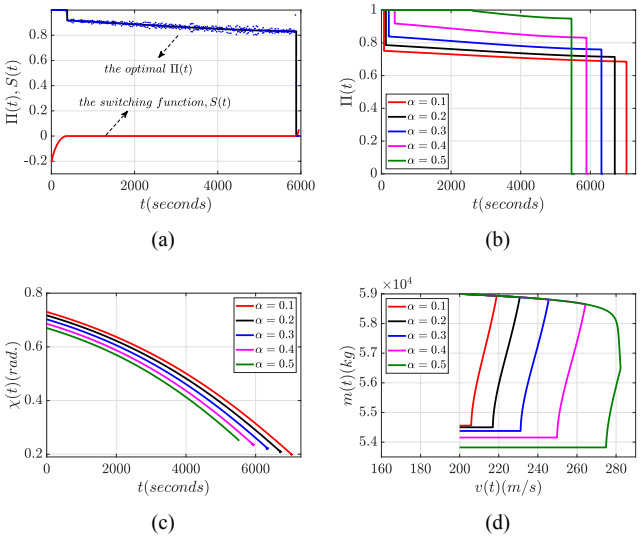

Fig. 1. (a): The optimal $\Pi(t)$ (black), and $S(t)$ (red) where $\alpha = 0.4$, compared to single-shooting Euler-based direct transcription method with 400 nodes (blue dots); The optimal cost by the direct method:**-30109.35**, The optimal cost by the indirect method:**-30109.38**. (b): The optimal $\Pi(t)$ in different α. (c): The optimal $\chi(t)$ in different α. (d): The optimal $m(t)$ as a function of $v(t)$ in different α.

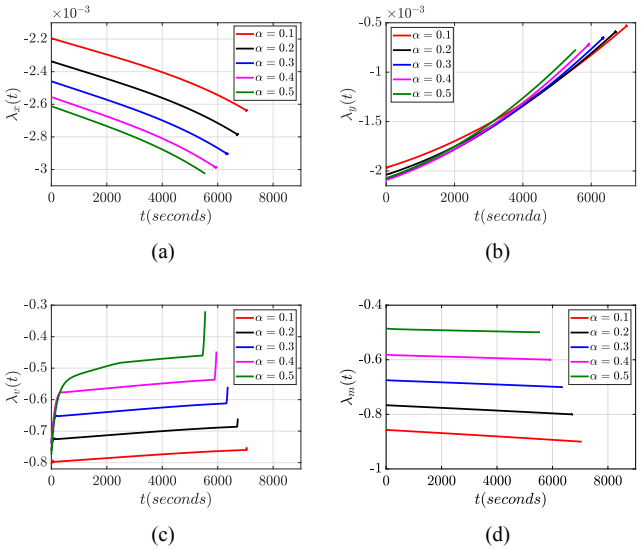

Fig. 2. (a): The optimal $\lambda_x(t)$ in different α. (b): The optimal $\lambda_y(t)$ in different α. (c): The optimal $\lambda_v(t)$ in different α. (d): The optimal $\lambda_m(t)$ in different α

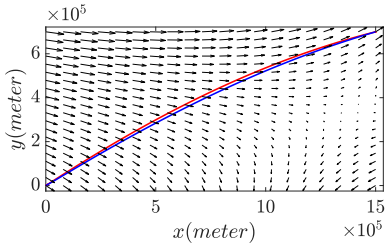

Fig. 3. The optimal $x - y$ trajectories (lateral path) in different α: blue and red lines show the lateral paths for $\alpha = 0.5$, and $\alpha = 0.1$ respectively.

REFERENCES

[1] Abolfazl Simorgh, Manuel Soler, Daniel González-Arribas, Sigrun Matthes, Volker Grewe, Simone Dietmüller, Sabine Baumann, Hiroshi Yamashita, Feijia Yin, Federica Castino, Florian Linke, Benjamin Lührs, and Maximilian Mendiguchia Meuser. A comprehensive survey on climate optimal aircraft trajectory planning. *Aerospace*, 9(3), 2022.

[2] Douglas M. Pargett and Mark D. Ardema. Flight path optimization at constant altitude. *Journal of Guidance, Control, and Dynamics*, 30(4):1197–1201, 2007.

[3] Damián Rivas and Alfonso Valenzuela. Compressibility effects on maximum range cruise at constant altitude. *Journal of Guidance, Control, and Dynamics*, 32(5):1654–1658, 2009.

[4] Antonio Franco, Damián Rivas, and Alfonso Valenzuela. Minimum-fuel cruise at constant altitude with fixed arrival time. *Journal of Guidance, Control, and Dynamics*, 33(1):280–285, 2010.

[5] Antonio Franco and Damián Rivas. Optimization of multiphase aircraft trajectories using hybrid optimal control. *Journal of Guidance, Control, and Dynamics*, 38(3):452–467, 2015.

[6] Antonio Franco and Damián Rivas. Analysis of optimal aircraft cruise with fixed arrival time including wind effects. *Aerospace Science and Technology*, 32(1):212–222, 2014.

[7] Banavar Sridhar, Hok K. Ng, and Neil Y. Chen. Aircraft trajectory optimization and contrails avoidance in the presence of winds. *Journal of Guidance, Control, and Dynamics*, 34(5):1577–1584, 2011.

[8] Hok K. Ng, Banavar Sridhar, and Shon Grabbe. Optimizing aircraft trajectories with multiple cruise altitudes in the presence of winds. *Journal of Aerospace Information Systems*, 11(1):35–47, 2014.

[9] A. E. Bryson and Y. C. Ho. Applied optimal control. *Taylor and Francis, Levittown, PA*, page Chap. 2, 1975.

[10] Mahya Aghaee and William W. Hager. The switch point algorithm. *SIAM Journal on Control and Optimization*, 59(4):2570–2593, 2021.

[11] H. Maurer, C. Büskens, J.-H. R. Kim, and C. Y. Kaya. Optimization methods for the verification of second order sufficient conditions for bang–bang controls. *Optimal Control Applications and Methods*, 26(3):129–156, 2005.

[12] G. Vossen. Switching time optimization for bang-bang and singular controls. *Journal of Optimization Theory and Applications*, 144:409–429, 2010.

[13] Rhonda Slattery and Yiyuan Zhao. Trajectory synthesis for air traffic automation. *Journal of Guidance, Control, and Dynamics*, 20(2):232–238, 1997.

[14] Michael R. Jackson, Yiyuan J. Zhao, and Rhonda A. Slattery. Sensitivity of trajectory prediction in air traffic management. *Journal of Guidance, Control, and Dynamics*, 22(2):219–228, 1999.

[15] Daniel González-Arribas, Manuel Soler, and Manuel Sanjurjo-Rivo. Robust aircraft trajectory planning under wind uncertainty using optimal control. *Journal of Guidance, Control, and Dynamics*, 41(3):673–688, 2018.

[16] Olivier Cots, Joseph Gergaud, and Damien Goubinat. Direct and indirect methods in optimal control with state constraints and the climbing trajectory of an aircraft. *Optimal Control Applications and Methods*, 39, 11 2017.

[17] D.H Jacobson, M.M Lele, and J.L Speyer. New necessary conditions of optimality for control problems with state-variable inequality constraints. *Journal of Mathematical Analysis and Applications*, 35(2):255–284, 1971.

[18] Richard F. Hartl, Suresh P. Sethi, and Raymond G. Vickson. A survey of the maximum principles for optimal control problems with state constraints. *SIAM Review*, 37(2):181–218, 1995.

[19] R. Gabasov and F. M. Kirillova. High order necessary conditions for optimality. *SIAM Journal on Control*, 10(1):127–168, 1972.

[20] D. Poles. Base of aircraft data (bada) aircraft performance modelling report. *EEC Technical/Scientific Report, Eurocontrol*, 2009.